Table S3, related to Figure 4, 5 and 6: Oligonucleotides used in this study.

OLIGONUCLEOTIDES	SOURCE	IDENTIFIER
TM54: 5'-GTATCCTCGTAGTGCAGATGTTTT-3'	FASMAC	N/A
TM55: 5'P-ATCGGACTGATTCGGTAGATCTG-3' (phosphorylation at the 5' end)	FASMAC	N/A
TM56: 5'-ATCGGACTGATTCGGTAGATCTG-3'	FASMAC	N/A
TM57: 5'-GTATCCTCGTAGTGCAGATGTTTTATCGGACTGATTCGGTAGATCTG-3'	FASMAC	N/A
TM58: 5'-CAGATCTACCGAATCAGTCCGATAAAACATCTGCACTACGAGGATAC-3'	FASMAC	N/A
TM60: 5'-GTATCCTCGTAGTGCAGATGTTTT-3'P (phosphorylation at the 3' end)	FASMAC	N/A
TM154: 5'-TTTTTTTTTTTTTTTTTTTTTTTTTTTTTTTTTTTTTTTTTTTTTTTT-3'	FASMAC	N/A
TM155: 5'-AAAAAAAAAAAAAAAAAAAAAAAAAAAAAAAAAAAAAAAAAAAAAA-3'	FASMAC	N/A
TM156: 5'-CCCCCCCCCCCCCCCCCCCCCCCCCCCCCCCCCCCCCCCCCCCCCC-3'	FASMAC	N/A
TM157: 5'-GGGGGGGGGGGGGGGGGGGGGGGGGGGGGGGGGGGGGGGGGGGGGG-3'	FASMAC	N/A
TM158: 5'-GATGGATGATGAATAAAGTGTGGGATGATCATGATGTATGGATAGGTTTTTTTTTTT-3'	FASMAC	N/A
TM159: 5'-GATGGATGATGAATAAAGTG-3'	FASMAC	N/A
TM160: 5'-GGGTTCGAAATCGATAAGCTTGGATCCAGAC-3'	FASMAC	N/A
TM182: 5'-GGAGGTGATAGCAATGCTTTCGTG-3'	FASMAC	N/A

TM165: 5’-IRD800-GATGGATGATGAATAAAGTGTGGGATGATCATGATGTATGGATAGGTTTTTTTTTTTT-3’	Integrated DNA Technologies	N/A
TM326: 5’- IRD800-TTTTTTTTTTTTTTTTTTTTTTTTTTTTTT-3’	Integrated DNA Technologies	N/A
M13 forward: 5’-GTAAAACGACGGCCAGTGA-3'	FASMAC	N/A
M13 reverse: 5'-AGGAAACAGCTATGACCAT-3'	FASMAC	N/A

Supplemental Figure 1

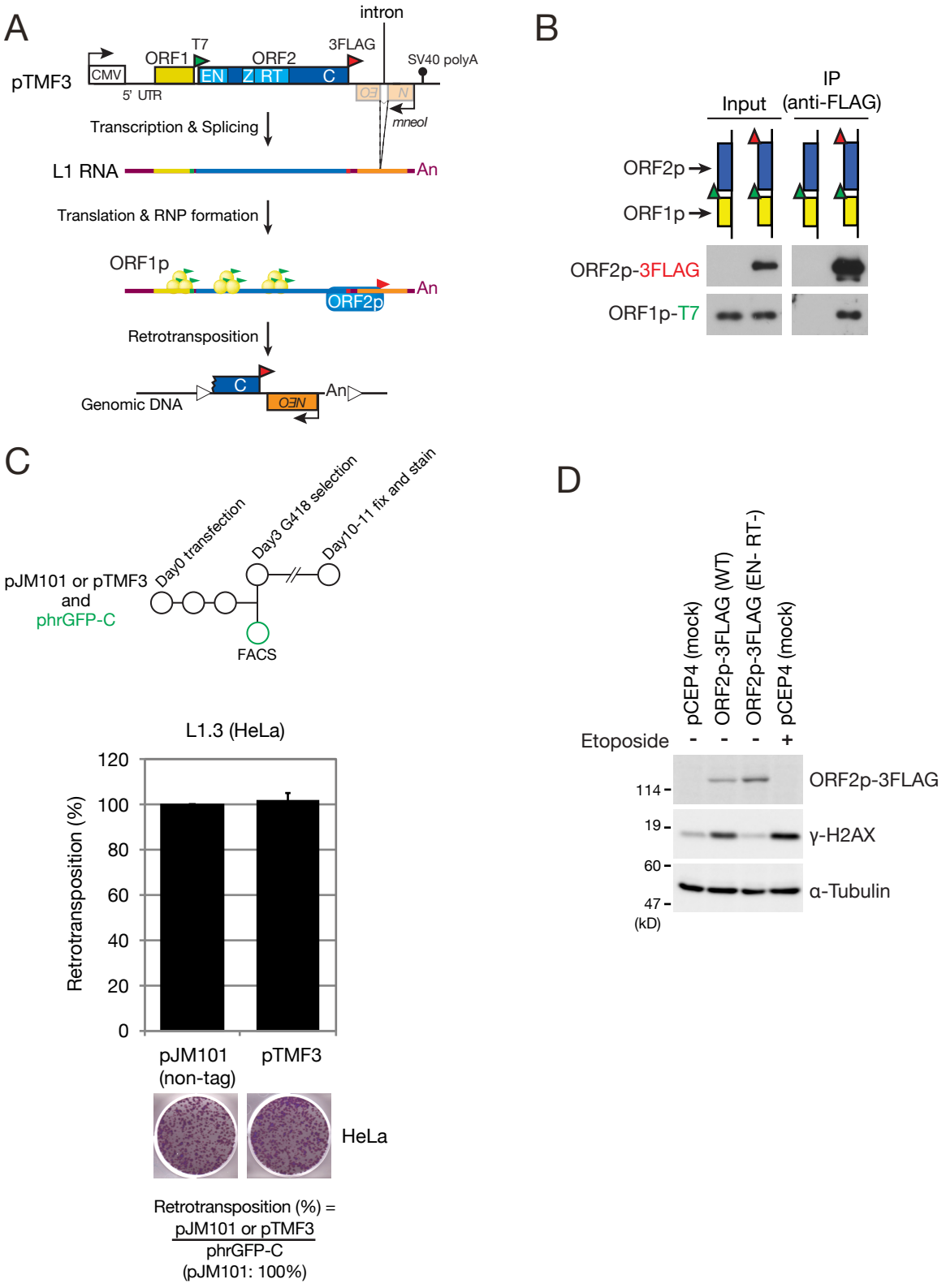

Supplemental Figure 2

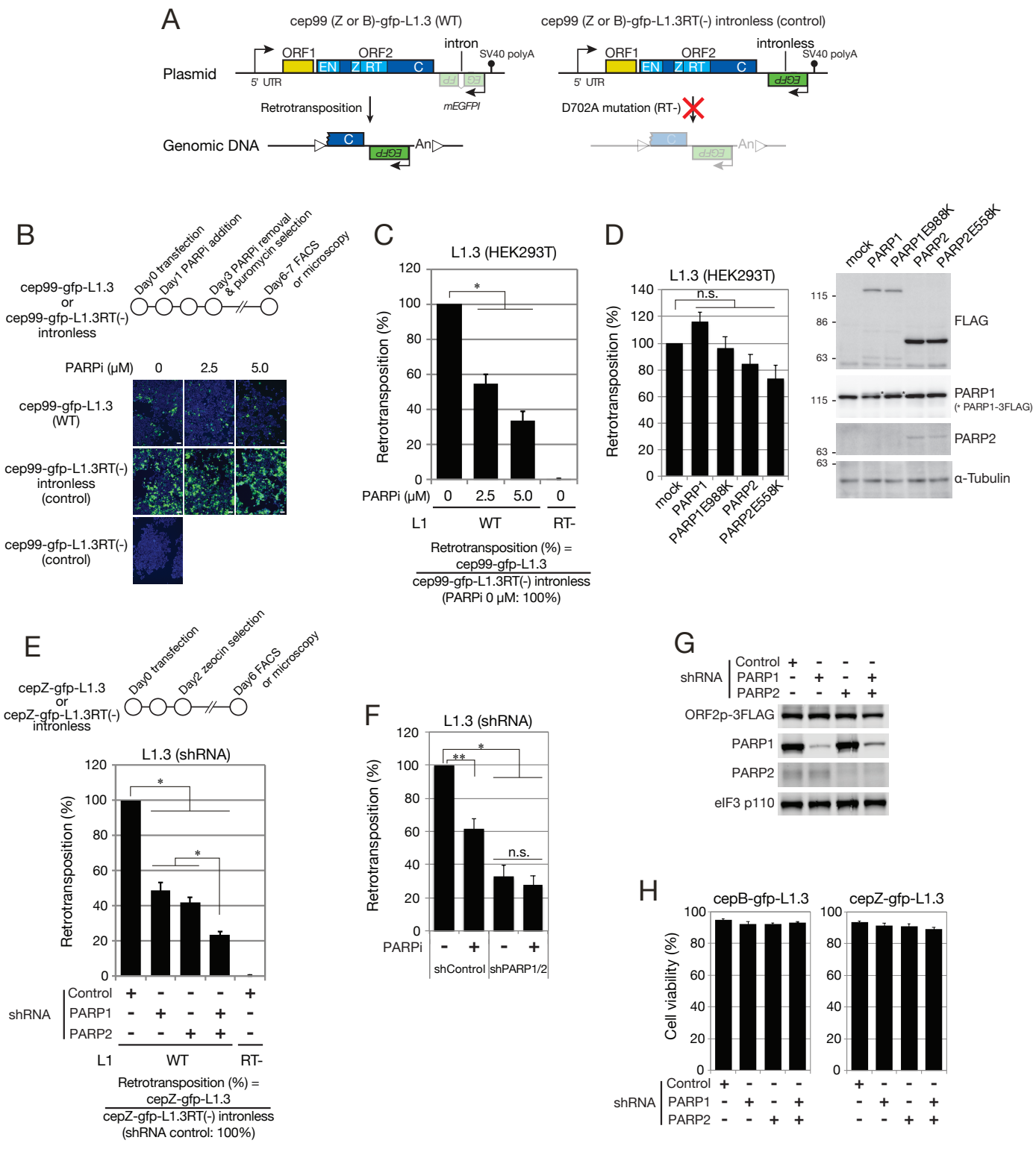

Supplemental Figure 3

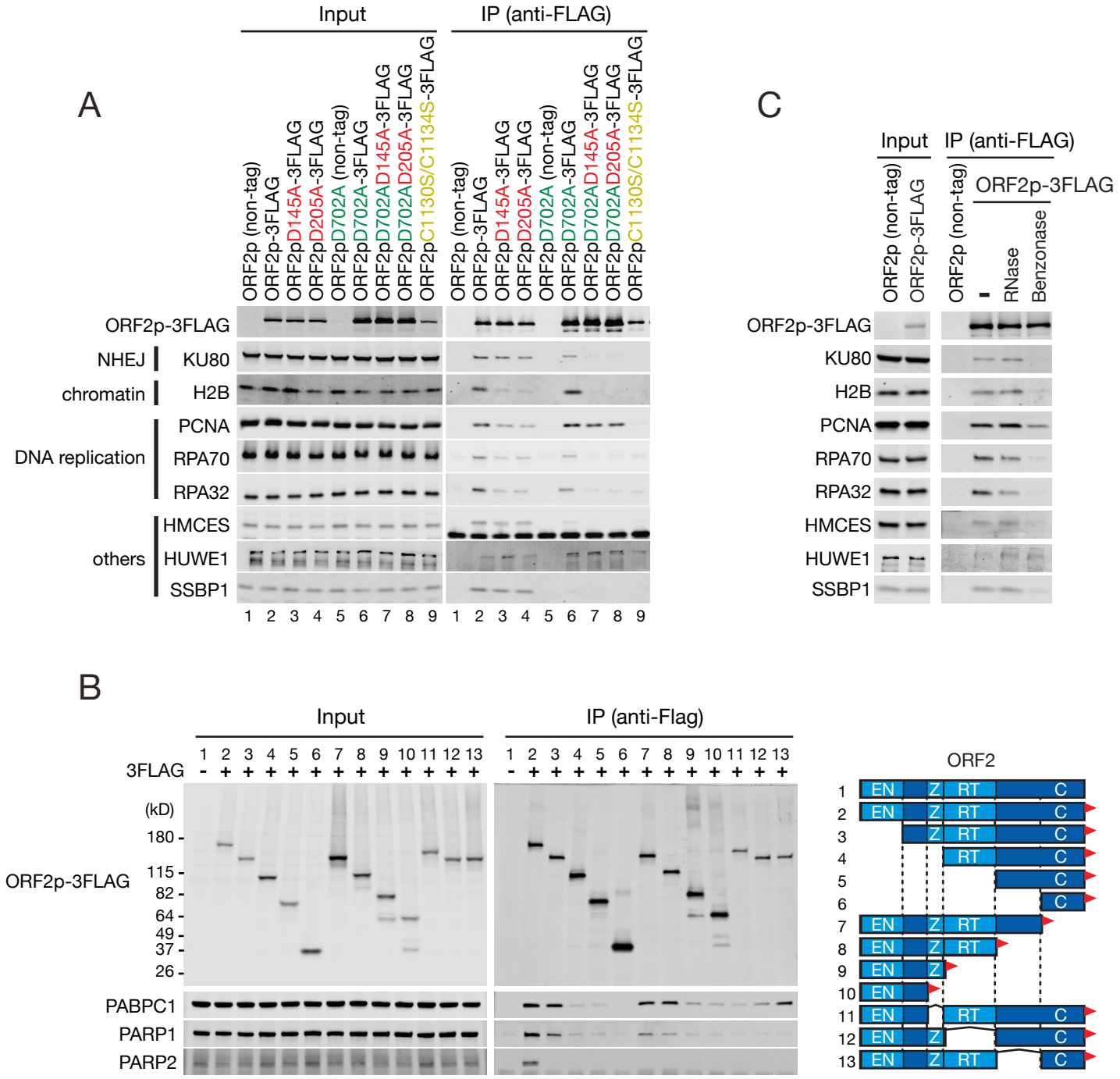

Supplemental Figure 4

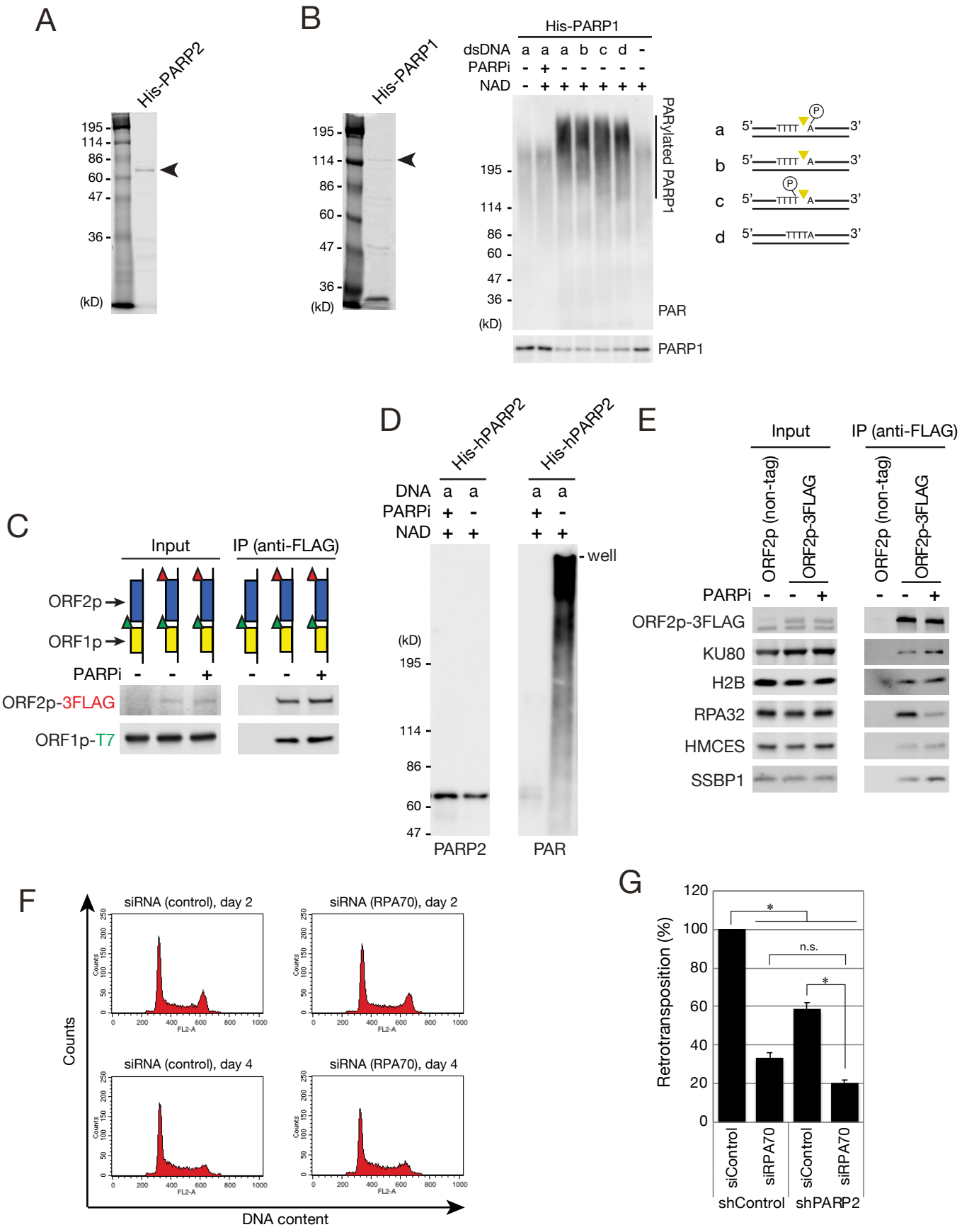

Supplemental Figure 5

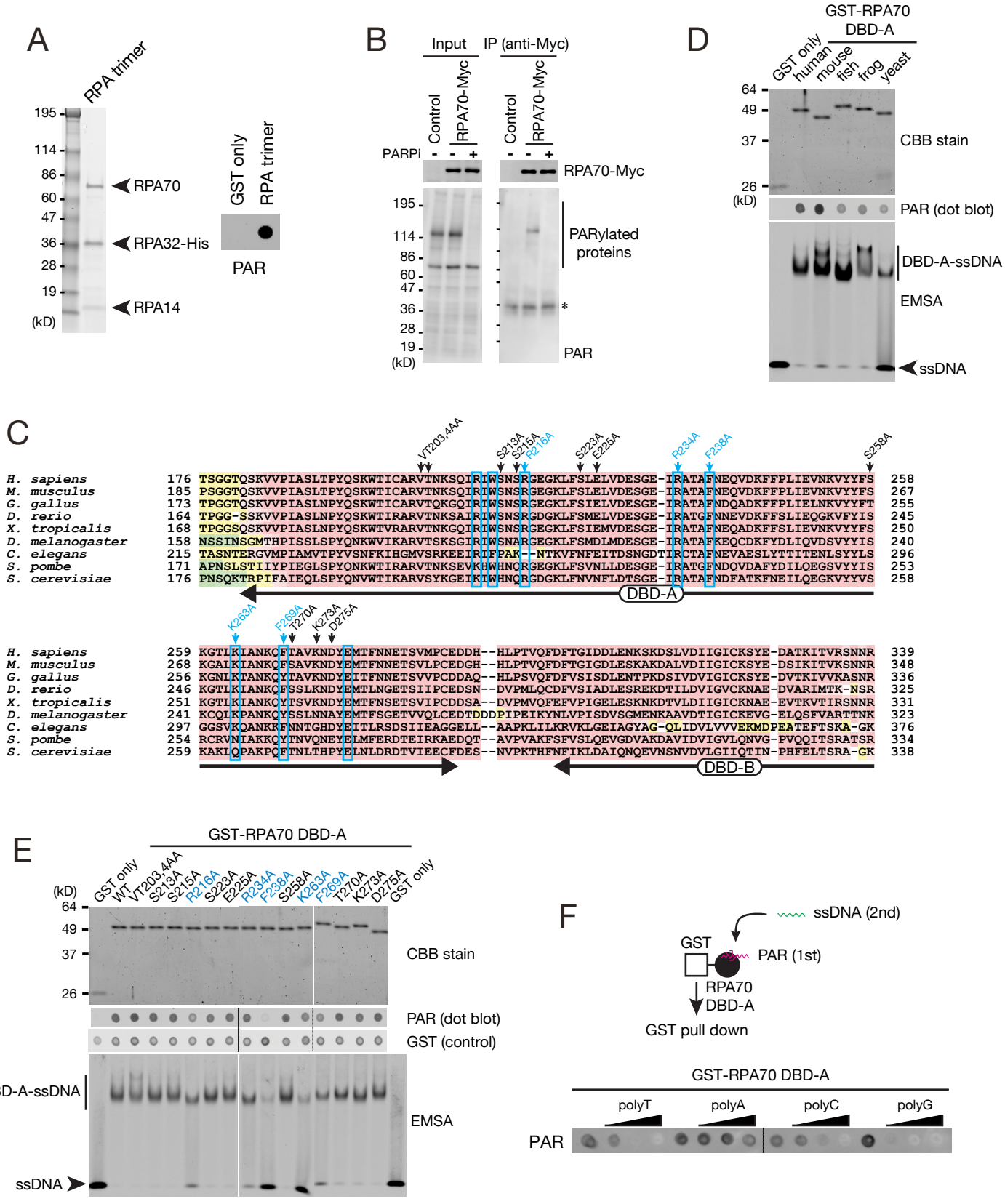

Supplemental Figure 6

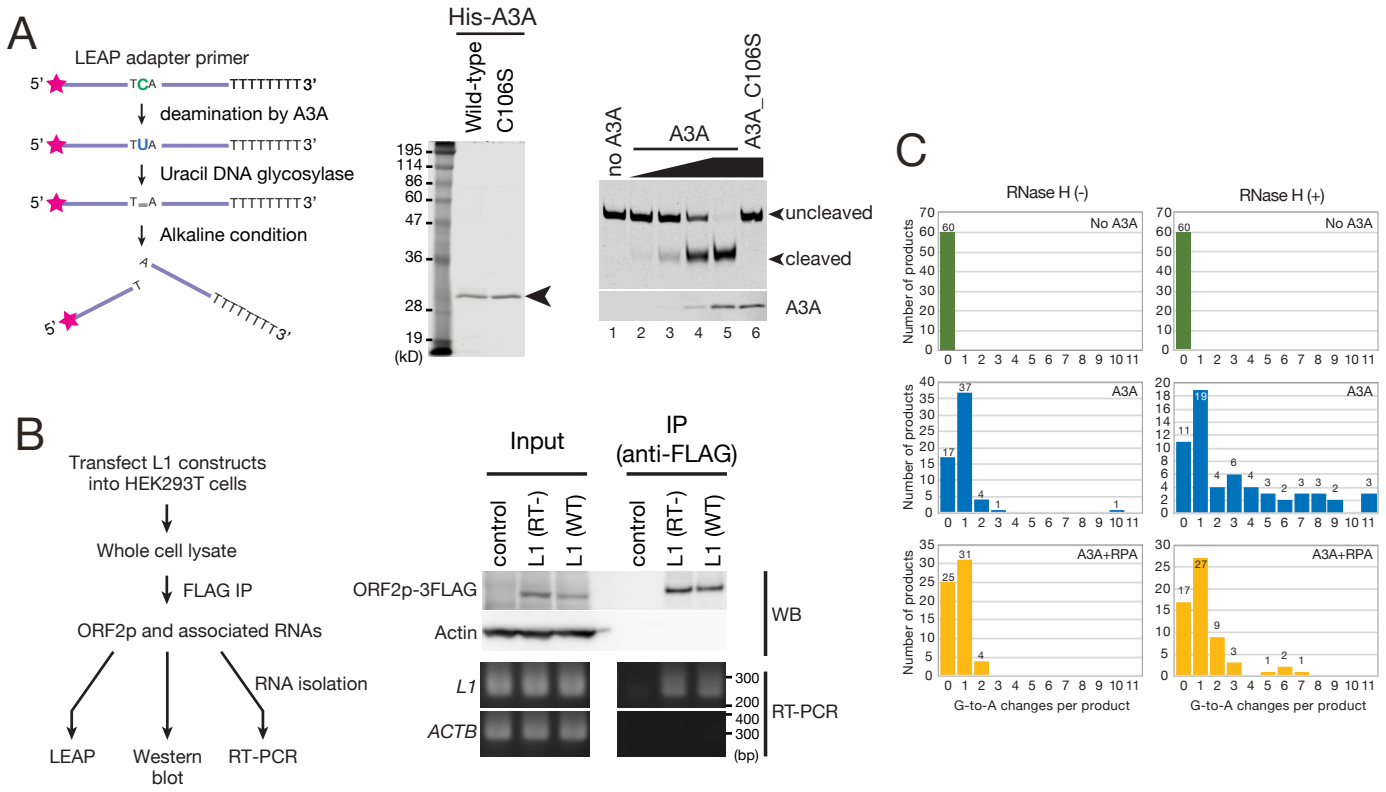

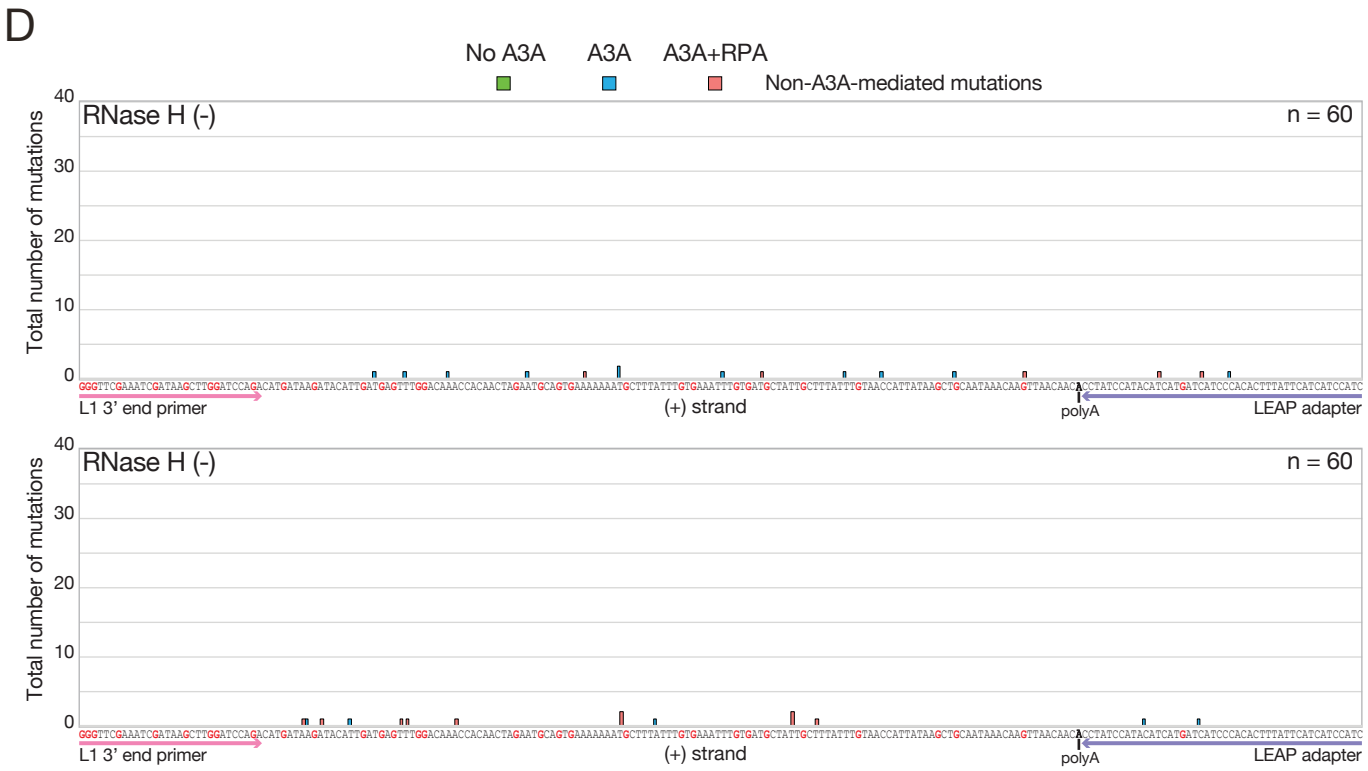

Supplemental Figure Legends

Figure S1, related to Figure 1: Characterization of L1 RNP formation and retrotransposition from an engineered L1 construct.

(A) A schematic of pTMF3. A human retrotransposition-competent L1 (L1.3) (Sassaman et al., 1997) was cloned into the pCEP4 episomal expression vector. A single in-frame T7 *gene10* (green triangle) or three copies of an in-frame FLAG (red triangle) epitope tag were inserted downstream of the *ORF1* or *ORF2* coding regions, respectively. A CMV promoter (black arrow) and the L1 5' UTR augments L1 expression. Also indicated is the SV40 polyadenylation signal (black lollipop) and the following regions in *ORF2*: EN, endonuclease domain; Z, Z domain; RT, reverse transcriptase domain; C, cysteine-rich domain. A backward copy of an *mneoI* retrotransposition indicator cassette (orange box) was inserted into the L1 3' UTR. The *mneoI* cassette is interrupted by an intron in the L1 transcriptional orientation. A successful round of retrotransposition, which involves the transcription of L1 RNA, splicing of the intron in the *mneoI* retrotransposition indicator cassette, and the reverse transcription/integration of an L1 cDNA into genomic DNA, allows activation of the neomycin phosphotransferase gene, conferring G418-resistance to cells. White triangles indicate target-site duplications (TSDs) presumed to flank the retrotransposed L1. "An" denotes an L1 poly(A) tract. Yellow circles with green rectangles indicate ORF1p-T7. A blue oval with a red triangle indicates ORF2p-3FLAG.

(B) Interaction of ORF1p-T7 and ORF2p-3FLAG. HEK293T cells were transfected with pDK101 (ORF1p-T7) or pTMF3 (ORF1p-T7 and ORF2p-3FLAG). The ORF2p-3FLAG complex was immunoprecipitated using anti-FLAG antibody-conjugated beads and western blots were preformed using anti-T7 and anti-FLAG antibodies. Input indicates whole cell lysates (~1.67%) used for immunoprecipitation. IP indicates immunoprecipitation reactions performed with anti-FLAG antibody-conjugated beads. Three biological replicates were performed for each experiment.

(C) Results of the retrotransposition assay. Top: the experimental timeline of the L1 retrotransposition assay. HeLa-JVM cells were co-transfected with either pJM101/L1.3 or pTMF3 and a green fluorescent protein expression vector (phrGFP-C). G418 selection began three days post-transfection. Bottom: The retrotransposition efficiency was calculated as the number G418-resistant foci after normalizing for the transfection efficiency by (*i.e.*, the percentage of GFP-positive cells). The x-axis indicates the construct name. The y-axis indicates the normalized retrotransposition efficiency. The assays conducted with pJM101/L1.3 are set at 100%. Standard errors (black error bar line) were calculated from three independent biological replicates. G418-resistant foci were fixed and visualized by crystal violet staining. A representative result from the retrotransposition assay is shown below the graph.

(D) γ-H2AX accumulation in the ORF2p-3FLAG expressing cells. HEK293T cells were transfected with the following constructs: (1) pCEP4 (mock); (2) pTMO2F3 (a monocistronic wild-type (WT) ORF2p-3FLAG expression vector); or (3) pTMO2F3D145AD702A (a monocistronic ORF2p-3FLAG expression vector that contains missense mutations in the EN and RT active sites (EN- RT-). Total cell lysates were prepared in the absence (-) or presence (+) of etoposide and subjected to western blotting using an anti-γ-H2AX antibody. The α-Tubulin protein served as a loading control. Molecular weight standards are shown at the left of the gel image.

Figure S2, related to Figure 2: Retrotransposition assays with the PARP inhibitor in HEK293T cells.

(A) Schematics of L1 constructs used in retrotransposition assays. Left: The rationale of the retrotransposition is described in Figure S1. The cep99-gfp-L1.3 construct contains a *mEGFPI* retrotransposition indicator cassette within its 3' UTR and a puromycin selectable marker in the pCEP4 plasmid backbone. A successful round of L1 retrotransposition results in EGFP-positive cells. The "Z" or "B" plasmid designations indicate the presence of a zeocin or blasticidin selectable marker in the pCEP4 plasmid background. Right: an L1 expression vector containing a missense mutation within the RT domain (cep99-gfp-L1.3 RT (-) intronless) cannot undergo retrotransposition. It contains an intronless version of an *EGFP* expression cassette within its 3'UTR. This L1 construct was used to normalize the transfection efficiency in each cell line.

(B) Results of the retrotransposition assay in HEK293T cells treated with the PARP inhibitor olaparib. Top: timeline of the assay. HEK293T cells were transfected with an L1 expression construct (cep99-gfp-L1.3) in the presence or absence of the PARP inhibitor. Puromycin selection began three days post-transfection. The intronless-*EGFP* containing plasmid (cep99-gfp-L1.3RT(-) intronless) was independently transfected into HEK293T cells to monitor transfection efficiency. Bottom: after selection, cells were fixed with paraformaldehyde and stained with 4', 6-diamidino-2-phenylindole (DAPI) to visualize nuclei. Green and blue signals indicate EGFP-positive cells and nuclei, respectively. White bar, 50 μm. The intronless-*EGFP* containing plasmid (cep99-gfp-L1.3RT(-) intronless) cannot undergo retrotransposition and was used to normalize the transfection efficiency in each cell line.

(C) Quantification of the L1 retrotransposition efficiency in HEK293T cells. Retrotransposition assays were conducted as described in panel B and puromycin resistant cells were subjected to flow cytometry six to seven days post transfection. The relative retrotransposition efficiencies were calculated by normalizing the number of EGFP-positive cells derived from cep99-gfp-L1.3

with the transfection control (cep99-gfp-L1.3RT(-) intronless). The x-axis indicates the PARP inhibitor concentrations and L1 constructs used in the assay. The y-axis indicates the normalized retrotransposition efficiency compared to the untreated control, which was set at 100%. Standard errors (black error bar lines) were calculated from three independent biological replicates. P-values were calculated using one-way ANOVA followed by Bonferroni multiple comparison test. An asterisk (*) indicates a p-value of < 0.005.

(D) Retrotransposition assays upon PARP1 or PARP2 overexpression. Left: HEK293T cells were transfected with an L1 expression construct (cep99-gfp-L1.3) and either a mock (pCMV-3Tag-9), PARP1 (PARP1/ pCMV-3Tag-9), PARP1E988K (PARP1E988K/ pCMV-3Tag-9), PARP2 (3FLAG C1-PARP2), or PARP2E558K (3FLAG C1-PARP2E558K) expression vector. Puromycin selection began two days post-transfection. The intronless-*EGFP* containing plasmid (cep99-gfp-L1.3RT(-) intronless) was independently transfected into HEK293T cells to monitor transfection efficiency. Puromycin resistant cells were subjected to flow cytometry six days post transfection. The relative retrotransposition efficiencies were calculated as in panel C. The x-axis indicates the ectopic PARP1 or PARP2 expression vectors used in the assay. The y-axis indicates the normalized retrotransposition efficiency compared to the control, which was set at 100%. Standard errors (black error bar lines) were calculated from three independent biological replicates. P-values were calculated by Bonferroni multiple comparison test. The notation “n.s.” means that the detection level was below the statistical threshold determined in the study (< 0.05). Right: Western blots of cell lysates using antibodies against the FLAG epitope tag, PARP1, or PARP2 were used to determine protein levels. The α-Tubulin protein served as a loading control.

(E) Retrotransposition assays in PARP1 and/or PARP2 shRNA-knockdown cells. Top: timeline of the assay. HEK293T cells were transfected with an L1 expression construct (cepZ-gfp-L1.3) containing an *mEGFPI*. Zeocin selection began two days post-transfection and zeocin resistant cells were subjected flow cytometry six days post transfection. Bottom: the relative

retrotransposition efficiencies were calculated by normalizing the number of EGFP-positive cells derived from cepZ-gfp-L1.3 with the transfection control (cepZ-gfp-L1.3RT(-) intronless). The x-axis indicates the shRNA cell lines and L1 constructs. The y-axis indicates the normalized retrotransposition efficiency compared to the non-mammalian shRNA control, which was set at 100%. Standard errors (black error bar lines) were calculated from nine independent biological replicates. P-values were calculated using one-way ANOVA followed by a Bonferroni multiple comparison test. Asterisks (*) indicates a p-value of < 0.005.

(F) Retrotransposition assays in PARP1 and PARP2 small hairpin RNA (shRNA)-knockdown cells treated with the PARP inhibitor. These assays were performed as described in panel C using cepB-gfp-L1.3 instead of cep99-gfp-L1.3 in the presence (5 μM olaparib) or absence of the PARP inhibitor. Blasticidin selection began three days post-transfection. The intronless-*EGFP* containing plasmid (cepB-gfp-L1.3RT(-) intronless) was independently transfected into HEK293T cells to monitor transfection efficiency. Blasticidin resistant cells were subjected to flow cytometry six to seven days post transfection. The relative retrotransposition efficiencies were calculated as in panel C. The x-axis indicates the shRNA cell lines used in the assay. The y-axis indicates the normalized retrotransposition efficiency compared to the untreated shRNA control, which was set at 100%. Standard errors (black error bar lines) were calculated from three independent biological replicates. P-values were calculated by Bonferroni multiple comparison test. An asterisk (*) or (**) indicates a p-value of < 0.005 or of < 0.05, respectively.

(G) ORF2p-3FLAG, PARP1 and PARP2 protein levels in shRNA-knockdown cells. The control (non-mammalian shRNA targeting), PARP1, PARP2, or PARP1/PARP2 (double knockdown) shRNA constructs were transduced in HEK293T cells using lentiviral vectors. These shRNA knockdown cell lines were then transfected with pTMO2F3. Western blots of cell lysates using antibodies against the FLAG epitope tag, PARP1, or PARP2 were used to determine protein levels. The elongation initiation factor 3 subunit (eIF3 p110) protein served as a loading control.

(H) Cell viability in shRNA-knockdown cells. The indicated shRNA knockdown cell lines subjected to retrotransposition assays in Figure 2D (cepB-gfp-L1.3) or S2E (cepZ-gfp-L1.3) were subjected to a Trypan blue (0.2%) exclusion assay. The X-axis indicates the cell lines. The Y-axis indicates the cell viability (%). Standard errors (black error bar lines) were calculated from five independent biological replicates.

Figure S3, related to Figure 3: Detailed analysis of the ORF2p-3FLAG complex.

(A) The association of ORF2p-3FLAG mutant proteins with other cellular proteins. The same samples used in Figure 3B were analyzed by western blotting using antibodies against the proteins indicated at the left of the gel images. The ORF2p-3FLAG lane is duplicated from Figure 3B (*i.e.*, it is the same image as the one shown in the top panel of Figure 3B) and serves as a reference. Input western blots lanes using approximately 1.67% of the whole cell lysate used in immunoprecipitation experiments. IP indicates immunoprecipitation reactions performed with anti-FLAG antibody-conjugated beads. A core histone subunit (H2B) exhibited an EN-dependent association with ORF2p-3FLAG. PCNA interacted with (EN-) and (RT-) ORF2p-3FLAG mutant proteins. Ku80, RPA70, RPA32, and HMCES exhibited a reduced interaction with the ORF2p-3FLAG (EN- RT-) double mutant proteins. HUWEI did not exhibit large differences in the association profiles with different mutant proteins. HMCES and SSBP1 did not interact strongly with the ORF2p-3FLAG RT mutant proteins, suggesting that it could potentially interact with newly synthesized L1 cDNAs. None of the proteins interacted strongly with an ORF2p-3FLAG protein containing mutations in the cysteine rich domain. Three biological replicates were performed for each experiment.

(B) Interaction of PARP1 and PARP2 with ORF2p-3FLAG deletion derivatives. HEK293T cells were independently transfected the following constructs: Lane 1, pAD001; Lane 2, pTMO2F3; Lane 3, pTMO2F3Z-C; Lane 4, pTMO2F3RT-C; Lane 5, pTMO2F3pRT-C; Lane 6, pTMO2F3C; Lane 7, pTMO2F3EN-pRT; Lane 8, pTMO2F3EN-RT; Lane 9, pTMO2F3EN-Z; Lane 10, pTMO2F3EN; Lane 11, pTMO2F3ΔZ; Lane 12, pTMO2F3ΔRT; or Lane 13, pTMO2F3ΔpRT (see STAR METHODS for plasmid information). Each ORF2p-3FLAG protein was purified and subjected to western blot analysis as described in Figure 1B. Schematics of the constructs are shown at the right of the gel images; red triangles indicate the positions of the FLAG-epitope tags. Input indicates western blots lanes using approximately 1.67% of the whole cell lysate used in

immunoprecipitation experiments. IP indicates immunoprecipitation reactions performed with anti-FLAG antibody-conjugated beads. There was no significant association between ORF2p-3FLAG and PARP1 with ORF2p-3FLAG mutant proteins lacking the central regions of ORF2p (lanes 11-13 on the anti-FLAG IP gel). None of the ORF2p-3FLAG mutant proteins could associate with PARP2. At least two biological replicates were performed for each experiment.

(C) Benzonase treatment significantly decreases interaction between ORF2p-3FLAG and a subset of host proteins. HEK293T cells were transfected with pTMO2F3 and the resultant ORF2p-3FLAG complexes were purified as in Figure 1B. Input indicates western blots lanes using approximately 1.67% of the whole cell lysate used for anti-FLAG immunoprecipitation reactions (IP). ORF2p-3FLAG complexes were immunoprecipitated in the absence or presence of RNase (A, I, and T1) or benzonase. Immunoprecipitation and western blots independently were performed using the samples presented in Figure 3C with antibodies against the proteins indicated at the left of the gel images. Most of the ORF2p-3FLAG interactions (*e.g.*, KU80, H2B, PCNA, RPA70, RPA32, HMCES, and SSBP1) were decreased upon benzonase treatment. Three biological replicates were performed for each experiment.

Figure S4, related to Figure 4: Effect of the PARP inhibitor treatment on the ORF2p complex formation.

(A) Recombinant PARP2 protein. A hexa-histidine-tagged PARP2 protein (His-PARP2) at its N-terminus was purified from *E. coli* extracts using TALON metal affinity resins, subjected to SDS-PAGE, and visualized by Coomassie Brilliant Blue (CBB) staining. The arrow indicates the position of His-PARP2. Molecular weight standards are indicated at the left of the gel image.

(B) *In vitro* PARP1 activation. Left: a hexa-histidine-tagged PARP1 protein at its N-terminus (His-PARP1) was purified from *E. coli* extracts using TALON metal affinity resins, subjected to SDS-PAGE, and visualized by Coomassie Brilliant Blue (CBB) staining. The arrow indicates the position of the His-PARP1 protein. Molecular weight standards are indicated at the left of the gel image. Middle: purified His-PARP1 was incubated with or without 20 μM NAD, 10 μM olaparib (PARPi), and 20 μM of a dsDNA substrate. Poly(ADP-ribosyl)ated-PARP1 was separated on an SDS-PAGE gel and detected by western blot using an anti-PAR antibody. The signals obtained with anti-PARP1 antibody served as a loading control. Right: schematics of the dsDNA substrates tested for PARP1 activation: (a) a 5’ phosphorylated nick; (b) an unphosphorylated nick; (c) a 3’ phosphorylated nick; and (d) a dsDNA lacking a nick. Gold triangles indicate the positions of the nick in the L1 ORF2p EN consensus cleavage sequence (5'-TTTT/A-3'). The 5' and 3' ends of the oligonucleotides used in the assay contain either a hydroxyl or phosphate group. An encircled “P” indicates the phosphate group.

(C) L1 RNP formation in the absence or presence of the PARP inhibitor. HEK293T cells were transfected with pDK101 or pTMF3 and treated with 10 μM olaparib (PARPi) for approximately 12 hours prior to cell collection. DMSO was added instead of olaparib as a negative control (PARPi (-)). The ORF2p-3FLAG complexes were prepared as described in Figure 1B and analyzed by western blotting using anti-FLAG or anti-T7 antibodies. HEK293T cells transfected with pDK101 (ORF1p-T7, ORF2p [non-tag]) served as a negative control. Input indicates western

blots lanes using approximately 1.67% of the whole cell lysate used in anti-FLAG immunoprecipitation reactions (IP). Two biological replicates were performed for each experiment.

(D) An anti-PARP2 antibody does not recognize PARylated-PARP2. PARP2 was activated by incubation with a double strand DNA substrate containing a 5' phosphorylated nick in either the presence or absence of 10 μM olaparib (PARPi) as described in Figure 4A. Western blots were preformed using an anti-PARP2 (left) or anti-PAR antibody (right).

(E) The effect of PARP inhibitor treatment on the other ORF2p-3FLAG host protein interactions. The same samples used in Figure 4B were analyzed by western blotting using antibodies against proteins listed at the left of the gel images. The ORF2p-3FLAG lane is duplicated from Figure 4B (*i.e.*, it is the same image from the top panel of Figure 4B). Only RPA32 exhibited a reduced association with ORF2p-3FLAG in the presence of the PARP inhibitor. Input indicates western blots lanes using approximately 1.67% of the whole cell lysate used for anti-FLAG immunoprecipitation reactions (IP). Three biological replicates were performed for each experiment.

(F) Cell cycle analysis of HEK293T cells transfected with RPA70 siRNAs. HEK293T cells transfected with siRNAs against RPA70 were fixed with ethanol, stained with propidium iodide (PI), and analyzed using a flow cytometer 2 and 4 days post-transfection. The x-axis indicates intensity of PI staining (DNA content). The y-axis indicates the cell number (Counts).

(G) Retrotransposition assays in RPA and PARP2 double knockdown cells. The indicated HEK293T cells were transfected with an L1 expression construct (cepB-gfp-L1.3) containing an *mEGFPI*-based retrotransposition indicator cassette in either the presence of a non-targeting siRNA (control) or a siRNA against RPA70. Blasticidin selection began two days post-transfection. Blasticidin resistant cells were subjected to flow cytometry six days post transfection. The relative retrotransposition efficiencies were calculated by normalizing the number of EGFP-positive cells derived from cepB-gfp-L1.3 with the transfection control (cepB-gfp-L1.3RT(-) intronless). The x-

axis indicates the shRNA knockdown cell lines and siRNA constructs used in the assay. The y-axis indicates the normalized retrotransposition efficiency compared to the shRNA control cells with siRNA control, which was set at 100%. Standard errors (black error bar lines) were calculated from three independent biological replicates. P-values were calculated using one-way ANOVA followed by a Bonferroni multiple comparison test. Asterisks (*) indicate a p-value of < 0.005.

Figure S5, related to Figure 5: OB-fold of RPA directly binds poly(ADP-ribose).

(A) RPA has high binding affinity for PAR. Left: the RPA subunits (RPA70, hexa-histidine-tagged RPA32 at its C-terminus [RPA32-His], and RPA14) were simultaneously expressed in bacteria. The RPA heterotrimer was purified using TALON metal affinity resins, subjected to SDS-PAGE, and visualized by CBB staining. The arrows indicate the positions of the RPA subunits. Molecular weight standards are indicated at the left of the gel image. Right: the recombinant RPA trimer was spotted onto a nitrocellulose membrane and incubated with PAR (PAR). After washing, membrane-associated PAR was detected using an anti-PAR antibody. The GST protein purified from bacteria served as a negative control.

(B) RPA70 association with PAR *in vivo*. HEK293T cells expressing RPA70 containing a Myc epitope tag at its carboxyl-terminus. The PARP inhibitor olaparib (10 μM PARPi [+]) or DMSO (PARPi [-]) was applied to media prior to cell collection. Input indicates western blots lanes using approximately 1.67% of the whole cell lysate used in anti-Myc immunoprecipitation reactions (IP). Anti-Myc and anti-PAR antibodies were used to detect RPA70-Myc and the co-precipitated PARylated proteins. Molecular weight standards are indicated at the left of the gel image. The asterisk denotes non-specific signals.

(C) Sequence alignments of the RPA DBD-A domains from various organisms. The RPA70 DBD-A domains were aligned using the Expresso alignment program based on structural similarities (http://www.tcoffee.org/Projects/expresso/) (Armougom et al., 2006). Red (pink), yellow, and green shading represent high, modest and poor agreements among the proteins, respectively. The numbers in each row indicate amino acid positions calculated from the methionine initiation codon. Thick black lines that end with arrows indicate the RPA70 DBD-A and DBD-B regions. Blue boxes indicate amino acid residues implicated in DNA recognition (Bochkarev et al., 1997). Vertical arrows indicate the position missense mutations examined in panel E (below) and Figure 5C.

(D) Conserved interactions between RPA70 DBD-A and PAR. Top: RPA70 DBD-A fragments from the indicated organisms were cloned into the GST expression vector (pGEX-2T). The N-terminal GST-tagged proteins were expressed in *E. coli* and purified using a glutathione sepharose. Middle: The recombinant GST-RPA DBD-A fusion proteins were subjected to the PAR binding assay described in Figure 5B. Bottom: Electrophoretic mobility shift assays (EMSA) were conducted by incubating the GST-RPA70 DBD-A fusion proteins with a single strand poly$(T)_{30}$ oligonucleotide labeled with IRDye800 at its 5' end (TM326). The ssDNAs (arrow) and GST-RPA70 DBD-A fusion protein/ssDNA complexes were separated on a polyacrylamide/Tris-borate-EDTA (TBE) gel. Human, *Homo sapiens*; mouse, *Mus musculus*; fish, *Danio rerio*; frog, *Xenopus tropicalis*; yeast, *Saccharomyces cerevisiae*.

(E) Mutant RPA70 DBD-A/PAR binding assays. Top: The recombinant GST-RPA70 DBD-A mutant fusion proteins were purified using glutathione sepharose. Middle: The purified GST-RPA70 DBD-A mutant fusion proteins were subjected to a PAR binding assay (STAR METHODS). After quantifying the PAR signal intensities, the anti-PAR antibody was stripped from the membrane, and western blotting was conducted using an anti-GST antibody to control for protein levels. Bottom: the purified GST-RPA70 DBD-A mutant fusion proteins were subjected to an electrophoretic mobility shift assay (EMSA) using the same methodology described in panel D. The ssDNAs (arrow) and GST-RPA70 DBD-A fusion protein/ssDNA complexes were separated on a polyacrylamide/Tris-borate-EDTA (TBE) gel. The dotted black lines indicate spliced boundaries between two different areas from the same membrane. Different gel images are separated by a white space.

(F) Single strand DNAs compete with PAR binding to RPA70 DBD-A. Top: GST-RPA70 DBD-A fusion protein was incubated with recombinant PAR in the absence or presence of single strand 50 nucleotide competitor DNAs. The resultant complexes then were subjected to GST-pull down

assays. Bottom: PAR/RPA70 DBD-A complexes formed in the absence or presence (10, 100 or 1,000 nM) of the indicated single strand competitor DNAs (polyT, TM154; polyA, TM155; polyC, TM156; polyG, TM157) were spotted onto a nitrocellulose membrane. PAR was detected by western blotting using an anti-PAR antibody. The dotted black line indicates a spliced boundary between two different areas from the same membrane.

Figure S6, related to Figure 6: RPA protects single strand DNA from DNA deamination.

(A) A3A deamination assay. Left: rationale of the assay. A single-strand LEAP adapter oligonucleotide labeled with IRDye800 at the 5' end (TM165) was incubated with recombinant A3A; deamination leads to a C-to-U mutation. The resultant uracil base is removed by treatment with uracil DNA glycosylase, leaving an abasic site. Incubation in alkaline conditions allows for cleavage of the abasic site. The magenta star indicates the IRDye label. The sequence 5'-TCA-3' is the A3A deamination consensus sequence. Middle: bacterially expressed N-terminal hexa-histidine-tagged human APOBEC3A (His-A3A) and an APOBEC3A (C106S) mutant protein were purified using TALON metal affinity resins, subjected to SDS-PAGE, and visualized by CBB staining. The arrows indicate the positions of the wild type and mutant proteins. Molecular weight standards are indicated at the left of the gel image. Right: the assay was conducted with the labeled LEAP adapter primer (5 nM) and the His-A3A recombinant protein (lanes 2-5, at two-fold concentration increase ranging from 15.625 to 125 nM). The His-A3A_C106S (125 nM) mutant protein served as a negative control. The signals were detected using the Odyssey CLx imaging system. The recombinant His-A3A protein was detected by western blotting using an anti-His antibody.

(B) Preparation of L1 RNPs for LEAP assay. Left: HEK293T cells were transfected with the following L1 expression constructs: (1) pJM101/L1.3 (control); (2) pTMF3 (WT ORF2p-3FLAG); or (3) pTMF3D702A (RT-). Whole cell lysates were prepared 4 days post-transfection. L1 RNPs were purified using an anti-FLAG antibody as described in Figure 1B. Aliquots of the purified L1 RNPs were used in LEAP, western blot, and RT-PCR experiments. Right: validation of L1 RNPs. ORF2p-3FLAG was detected in both whole cell lysates (input) and IP reactions using an anti-FLAG antibody. L1 RNA was detected in whole cell lysates and IP reactions by RT-PCR. β-Actin (*ACTB*) served as a negative control.

(C) Analysis of LEAP products. The sixty LEAP products analyzed in Figure 6C were used to indicate the number of G-to-A changes in a “single” LEAP product. LEAP reactions were conducted in the absence (left) or presence (right) of RNase H. The x-axis indicates the number of G-to-A changes in the (+) strand L1 cDNA product. The y-axis indicates the number of LEAP products. When RPA is added to the reaction, there are fewer G-to-A changes in the (+) strand L1 cDNA product, suggesting that RPA inhibits A3A-mediated cytosine deamination.

(D) Sequence analysis of LEAP products for non-A3A-mediated mutations. The sixty LEAP products analyzed in Figure 6C were used to indicate non-A3A-mediated mutations. LEAP reactions were conducted in the absence (top) or presence (bottom) of RNase H. Reactions were conducted in the absence of A3A (green rectangles), the presence of A3A (blue rectangles), or the presence of both A3A and RPA (red rectangles). The x-axis indicates the (+) strand L1 cDNA LEAP sequence. Guanine nucleotides are shown in red. Sequences underlined with pink and purple denote the L1 3’ end primer (TM160) and LEAP adapter primer (TM158), respectively. The outlined letter “A” indicates the position of the variably sized poly(A) tract in the LEAP products. The y-axis indicates the total number of non-A3A-mediated (non G-to-A) mutations in the LEAP products.